# 

Cite as: Appl. Phys. Lett. 118, 112104 (2021); https://doi.org/10.1063/5.0042857 Submitted: 04 January 2021 • Accepted: 03 March 2021 • Published Online: 16 March 2021

🗓 M. Hayden Breckenridge, 🗓 Pegah Bagheri, 🗓 Qiang Guo, et al.

## COLLECTIONS

F This paper was selected as an Editor's Pick







#### ARTICLES YOU MAY BE INTERESTED IN

MBE growth and donor doping of coherent ultrawide bandgap AlGaN alloy layers on single-crystal AlN substrates

Applied Physics Letters 118, 092101 (2021); https://doi.org/10.1063/5.0037079

Shallow Si donor in ion-implanted homoepitaxial AIN Applied Physics Letters 116, 172103 (2020); https://doi.org/10.1063/1.5144080

Carrier trapping and recombination at carbon defects in bulk GaN crystals grown by HVPE Applied Physics Letters 118, 112105 (2021); https://doi.org/10.1063/5.0040641





## 

Cite as: Appl. Phys. Lett. **118**, 112104 (2021); doi: 10.1063/5.0042857 Submitted: 4 January 2021 · Accepted: 3 March 2021 · Published Online: 16 March 2021







M. Hayden Breckenridge,<sup>1,a)</sup> Degah Bagheri, Dalar Guo, Dalar Biplab Sarkar, Dolar Khachariya, Dolar Khachariya, Dolar Khachariya, Dalar K

### **AFFILIATIONS**

- Department of Material Science and Engineering, North Carolina State University, Raleigh, North Carolina 27606, USA
- <sup>2</sup>Department of Electrical and Computer Engineering, North Carolina State University, Raleigh, North Carolina 27606, USA
- <sup>3</sup>Adroit Materials, Cary, North Carolina 27518, USA

#### **ABSTRACT**

We demonstrate Si-implanted AlN with high conductivity (>1  $\Omega^{-1}$  cm<sup>-1</sup>) and high carrier concentration (5 × 10<sup>18</sup> cm<sup>-3</sup>). This was enabled by Si implantation into AlN with a low threading dislocation density (TDD) (<10<sup>3</sup> cm<sup>-2</sup>), a non-equilibrium damage recovery and dopant activation annealing process, and *in situ* suppression of self-compensation during the annealing. Low TDD and active suppression of  $V_{Al}$ -nSi<sub>Al</sub> complexes via defect quasi Fermi level control enabled low compensation, while low-temperature, non-equilibrium annealing maintained the desired shallow donor state with an ionization energy of ~70 meV. The realized n-type conductivity and carrier concentration are over one order of magnitude higher than that reported thus far and present a major technological breakthrough in doping of AlN.

Published under license by AIP Publishing. https://doi.org/10.1063/5.0042857

Aluminum nitride (AlN) provides an attractive opportunity for the development of next-generation power electronic and deep-UV optoelectronic devices due to its large bandgap of 6.1 eV, Schottky barriers > 2 eV, and breakdown fields greater than 15 MV cm<sup>-1</sup>.<sup>1-5</sup> In order to demonstrate highly conducting regions for optoelectronics and low doped drift regions for power electronics, doping and compensation must be controlled over several orders of magnitude. However, the achievable free electron concentration in homoepitaxial Si-doped AlN is currently limited to concentrations <10<sup>16</sup> cm<sup>-3</sup> at room temperature.<sup>6,7</sup> The carrier concentration is limited partly by compensation by high threading dislocation densities (TDDs).8,9 AlN films are typically grown on foreign substrates (e.g., sapphire or SiC) with TDDs  $\geq 10^8 \, \text{cm}^{-2}$ ,  $^{10-13}$ compensating vacancy-Si complexes, 9,14 and the formation of an Si DX center is accompanied by high activation energy.<sup>6</sup> Consequently, obtaining highly conducting AlN requires reducing TDDs, vacancy complexes, and addressing the formation of the DX center.

AlN films grown by MOCVD on AlN single crystal substrates have been shown to have TDDs  $< 10^3\,\mathrm{cm}^{-2}$ , making the TDD-related compensation negligible. As a recent breakthrough, we have demonstrated that ion implanted Si can remain in the shallow donor state

 $(d^{0'+})$ , with an ionization energy of  $\sim$ 70 meV, rather than relaxing into the deep DX state after damage recovery and dopant activation annealing. This was realized by employing a relatively low annealing temperature  $(1200\,^{\circ}\text{C})$  to recover the lattice damage, preventing the system from reaching thermodynamic equilibrium, and forming an energetically favorable deep DX acceptor state. However, utilizing higher annealing temperatures and driving the system closer to the equilibrium resulted in the DX formation and low conductivities, similar to those observed for epitaxially doped AlN. However, similar to doping during the epitaxial growth, damage recovery and dopant activation annealing processes led to high self-compensation, resulting in over an order of magnitude lower conductivity than that expected based on the low ionization energy. Hence, controlling the formation of these compensating point defects seems to be the last obstacle in attaining higher free electron concentrations in Si-doped AlN.

In this work, we expand on our previous demonstration of shallow ( $\sim$ 70 meV) Si doping in low TDD AlN by ion implantation where we showed that ion implantation, as a non-equilibrium process, may provide an avenue to manage the population distribution between the two possible Si states in AlN: a shallow donor and a deep acceptor. <sup>18</sup> In the current work, we implement *in situ* control of point defects to suppress self-compensation during the recovery and activation

a) Author to whom correspondence should be addressed: mhbrecke@ncsu.edu

annealing process. The non-equilibrium annealing process in combination with *in situ* point defect control enabled us to realize more than one order of magnitude higher free carrier concentration than possible before.

In general, the concentration of a point defect that readily incorporates into a crystal depends upon its formation energy, which can be expressed as<sup>20</sup>

$$E^{f}(X^{q}) = E_{ref}(X^{q}) - \sum_{j} n_{j}\mu_{j} + q(E_{F} + E_{V}),$$
 (1)

where  $E_{ref}$  is the free energy of a crystal with a single defect referenced to the free energy of an ideal crystal,  $n_i$  is the number of atoms of the j-th-type exchanged with the reservoir to form the defect,  $\mu_i$  is the associated chemical potential, and  $E_F$  is the Fermi energy referenced with respect to the valence band maximum,  $E_V$ . From this relationship, there are two paths by which defect incorporation can be controlled: (1) chemical potential, wherein one controls process conditions<sup>21–26</sup> in order to influence corresponding impurities or host chemical potentials to lower the overall defect formation energy, 27,28 and (2) defect Quasi Fermi Level (dQFL), where the QFL associated with each defect is modified by introducing excess minority carriers into the system during the process, <sup>29–36</sup> which increases defect's formation energy and decreases its population. A comprehensive study and theoretical framework for the latter approach can be found elsewhere.<sup>29</sup> While we have demonstrated the dQFL for epitaxial growth, we hypothesize that the same approach, i.e., generation of minority carriers by above bandgap illumination, can be as effective in the damage recovery and dopant activation annealing process.

Low dislocation density ( $<10^3 \, \mathrm{cm}^{-2}$ ) AlN single crystal substrates processed from AlN boules grown by physical vapor transport were used in this study. AlN homoepitaxial films were grown via metal organic chemical vapor deposition (MOCVD) at a temperature of 1100 °C and a total pressure of 20 Torr. The V/III ratio of 1000 was established by flowing 8.4  $\mu$ mol/min of trimethylaluminum (TMA) and 0.3 slm of ammonia (NH<sub>3</sub>) at a total flow rate of 10 slm with hydrogen as a diluent gas. Further details pertaining to AlN homoepitaxial growth are described elsewhere. Si was then implanted into the homoepitaxial AlN film at room temperature with a dose of  $1 \times 10^{14}$  atoms/cm<sup>2</sup> and an acceleration voltage of 100 keV. The AlN films were implanted with a tilt angle of 7° to reduce the effects of channeling during ion implantation.

The optical properties of the AlN films were characterized by photoluminescence spectroscopy (PL) at room temperature using a 193 nm ArF excimer laser with a pulse width of 5 ns, a repetition rate of 100 Hz, and a power density of  $\sim\!\!5\,\mathrm{kW/cm^2}$ . Optical spectra were dispersed using a Princeton Instruments Acton SP2750 0.75 m high-resolution spectrograph with a 3200 grooves/mm optical grating and detected using a PIXIS: 2KBUV Peltier-cooled charge-coupled device camera.

Post-implantation annealing was performed at  $1200\,^{\circ}\text{C}$  for  $120\,\text{min}$  in a nitrogen atmosphere and a pressure of  $100\,\text{Torr}$ . The above bandgap UV-illumination during the annealing was implemented by a  $1\,\text{kW}$  Hg-Xe lamp (Oriel 6293) with a measured power density of  $1\,\text{W/cm}^2$  at the sample surface. Further details about the lamp setup are described elsewhere. V/Al/Ni/Au ( $30/100/70/70\,\text{nm}$ ) contacts  $^{42,43}$  in the van der Pauw geometry were deposited onto the surface of samples by electron beam evaporation as described elsewhere. The electrical contacts were annealed via rapid thermal

annealing at  $850\,^{\circ}$ C for  $60\,s$  in a nitrogen atmosphere. The carrier type, free electron concentration, and electron mobility were determined using an 8400 series LakeShore AC/DC Hall measurement system performed at elevated temperatures (> $400\,^{\circ}$ C). The AC Hall measurements were performed using a magnetic field and excitation frequency of  $\sim 0.62\,\mathrm{T}$  and  $100\,$  mHz, respectively. Temperature-dependent ( $300-725\,\mathrm{K}$ ) conductivity measurements were obtained using an Ecopia HMS-5500 and contacts in the van der Pauw configuration.

It was previously reported that annealing of Si-doped AlN at a temperature of 1200 °C for implantation damage recovery led to a lower donor ionization energy ( $E_i \sim 70 \, meV$ ), with only the shallow donor state d<sup>0/+</sup> observed, suggesting that the deep DX formation was inhibited.<sup>18</sup> Despite this lower ionization energy and approximately one order of magnitude increase in conductivity at room temperature compared to epitaxially doped AlN:Si, significant compensation was observed, which resulted in much lower electrical conductivity than that expected from the low ionization energy. The presence of compensating point defects after the damage recovery and dopant activation process was confirmed by the room temperature PL, showing broad midgap luminescence peaks associated with V<sub>Al</sub>-nSi<sub>Al</sub>. Similar midgap luminescence and compensation were observed in epitaxially doped films. We demonstrated more than one order of magnitude reduction in these compensating defects by active point defect control during the growth via minority carrier generation.<sup>32</sup> A similar process utilizing the above bandgap illumination was applied here during the post-implantation annealing. Figure 1 shows midgap luminescence spectra for Si-implanted AlN samples annealed under dark (red) and illuminated (blue) conditions. A significant (more than one order of magnitude) reduction in the midgap luminescence is observed for the UV-annealed samples in comparison to the annealing under dark conditions, which suggests a significant suppression of the V<sub>Al</sub>-nSi<sub>Al</sub>-related point defects, which have been identified as compensators in Si-doped AlN. 45

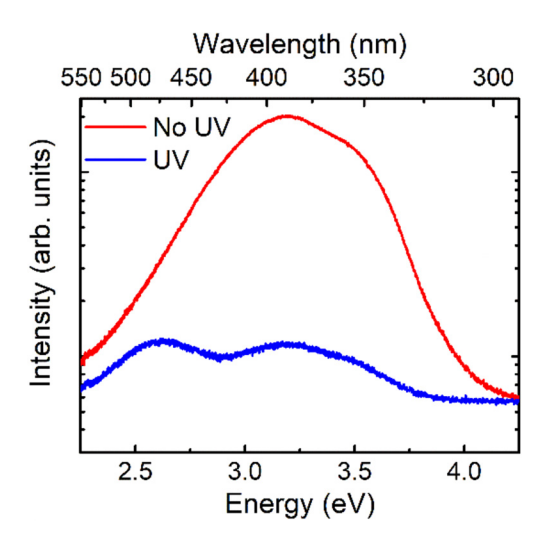


**FIG. 1.** Room temperature photoluminescence spectra for Si-implanted AIN annealed without (red) and with (blue) UV illumination, showing more than one order of magnitude reduction in V<sub>AI</sub>-nSi<sub>AI</sub>-related point defects. The spectra were normalized with respect to the band edge luminescence to facilitate direct comparison of the midgap luminescence peaks.

Identifying the main point defects associated with the deep luminescence allows for a prediction of their corresponding decrease based on the dQFL control framework. The procedure to determine the expected decrease in the defect concentration for a specified defect at a given illumination intensity is described in detail elsewhere.<sup>29,47</sup> For the estimation, V<sub>Al</sub>-2Si<sub>Al</sub> point defects in specific charge states consistent with the measured midgap luminescence spectra were considered. 45,46 Using the Varshni equation and the fitting parameters for AlN, we estimate the bandgap of AlN at the annealing temperature (1200 °C) to be  $\sim$ 4.9 eV. The experimental work of Reddy et al. shows that the Fermi level for AlN is pinned at ~2.7 eV below the conduction band minimum. Assuming that the barrier height scales with the bandgap, 1,2,48 we estimate a barrier height of  $\sim$ 2.2 eV at the annealing temperature, <sup>49</sup> which estimates the Fermi level at the annealing temperature of  $\sim$ 2.7 eV above the valence band. Using the estimated Fermi level, a process efficiency of ~90% and a reduction in the compensating defect population of around an order of magnitude are expected for samples annealed with the above bandgap illumination as compared to the samples annealed under dark conditions. This estimate roughly corresponds to the observed midgap PL intensity decrease in Fig. 1.

Electrical conductivity as a function of temperature for Si-implanted AlN annealed with and without above bandgap illumination is shown in Fig. 2. Interestingly, the sample annealed with UV-illumination without reaching equilibrium conditions (1200 °C, blue) exhibited a similar slope to the sample annealed without dQFL control (red) but showed about 30 times higher conductivity across the whole temperature range. This inferred that the shallow donor ( $E_i \sim 70 \, \mathrm{meV}$ ) state was maintained and was determined by the process kinetics rather than illumination. For comparison, the conductivity data for Si-implanted AlN samples annealed at higher temperatures (1400 and 1500 °C) under dark conditions show a much higher ionization energy ( $E_i \sim 290 \, \mathrm{meV}$ ),  $^{18}$  comparable to the ionization energy reported for the epitaxially doped AlN. The  $\sim 30$ -fold increase in conductivity is consistent with the predictions of the dQFL

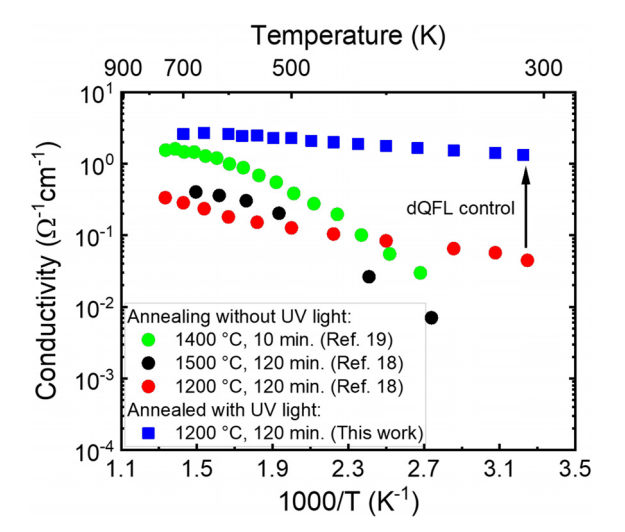


**FIG. 2.** Temperature-dependent conductivities for Si implanted AIN samples annealed without UV light:  $1400\,^{\circ}\text{C}$  for  $10\,\text{min}$  (green circles),  $^{19}$   $1500\,^{\circ}\text{C}$  for  $120\,\text{min}$  (black circles),  $^{18}$  and  $1200\,^{\circ}\text{C}$  for  $120\,\text{min}$  (red circles);  $^{18}$  the sample annealed with UV light  $1200\,^{\circ}\text{C}$  for  $120\,\text{min}$  (blue squares).

model and the observed reduction in compensator-related midgap photoluminescence intensity.

To estimate the compensation ratio  $(N_a/N_d)$  for the two annealing conditions, the conductivity,

$$\sigma = ne\mu,$$
 (2)

can be used, where n is the number of free electrons, e is the electron charge, and  $\mu$  is the electron mobility. Since the conductivity change with temperature in semiconductors is dominated by the change in the free carrier concentration, a charge balance model that relates free carriers to temperature can be expressed by the following equation:

$$n = \frac{1}{2} \left[ -\left( N_a + \frac{1}{g} N_C \exp\left( -\frac{\Delta E_i}{k_B T} \right) \right) + \sqrt{\left( N_a + \frac{1}{g} N_C \exp\left( -\frac{\Delta E_i}{k_B T} \right) \right)^2 + \frac{4}{g} N_C (N_d - N_a) \exp\left( -\frac{\Delta E_i}{k_B T} \right)} \right],$$
(3)

where  $N_a$  and  $N_d$  are the acceptor and donor concentrations, respectively,  $N_C$  is the density of states in the conduction band, g is the charge degeneracy factor, T is the temperature,  $E_i$  is the ionization energy (70 meV), and  $k_B$  is Boltzmann's constant. The compensation ratios for the samples annealed under dark and illuminated conditions were calculated by fitting Eq. (3) to be 0.9 and 0.2, respectively. The obtained reduction in compensation is again consistent with the predicted value, PL results, and increase in conductivity.

The carrier type was confirmed to be *n*-type via the hot probe and AC Hall measurements. The Gaussian implants with the carrier concentration and mobility varying with the depth introduced difficulties in achieving reliable low temperature Hall measurements, which require uniform profiles and properties. However, at temperatures above 400 °C, reproducible Hall measurements were obtained, and the measured free electron concentration and mobility were  $\sim$ 5 × 10<sup>18</sup> cm<sup>-3</sup> and  $\sim$ 1 cm<sup>2</sup>/V s, respectively, assuming uniform properties over a thickness of 200 nm. Hence, the measured sheet carrier concentration of  $1 \times 10^{14}$  cm<sup>-2</sup> for the sample with the dQFL was comparable to the original Si dose implanted into the film. This result indicates that nearly all the Si atoms were activated and promoted to the Al-substitutional sites. Based on the estimated compensation ratio of 0.2 and  $N_d\text{-}N_a$  of  $\sim\!\!5\times10^{18}~\text{cm}^{-3}$  in the sample illuminated with UV light, we estimate the donor and acceptor concentrations to be  $\sim$ 6 × 10<sup>18</sup> and 1 × 10<sup>18</sup> cm<sup>-3</sup>, respectively. The sample annealed without the dQFL had approximately one order of magnitude lower sheet carrier concentration  $\sim 10^{13}$  cm<sup>-2</sup> at a similar mobility. <sup>18</sup> Based on the estimated compensation ratio of 0.9 for the sample that did not receive the UV light, we estimate the donor and acceptor sheet concentrations to be  $\sim 1.1 \times 10^{14}$  and  $\sim 1 \times 10^{14}$  cm<sup>-3</sup>, respectively.

This highlights the utility of dQFL control and its ability to significantly reduce compensation during the post implantation damage recovery and activation annealing process. Although a high conductivity exceeding 1  $\Omega^{-1}\,\text{cm}^{-1}$  at room temperature was demonstrated in AlN by ion implantation, the measured carrier mobility was about 100 times lower than that can be achieved in the epitaxial doping despite the low compensation ratio. This phenomenon requires further investigation.

In conclusion, we have demonstrated a viable process for achieving high sheet conductance and high free carrier concentration in homoepitaxially grown, Si-implanted AlN. This was enabled by three key process advancements: (1) growth of AlN with the TDD  $<10^3\,\mathrm{cm}^{-2}$ , (2) maintaining the Si dopant in a shallow state by a non-equilibrium annealing process, and (3) suppressing self-compensation via  $V_{\mathrm{Al}}\text{-nSi}_{\mathrm{Al}}$  complexes by dQFL control. The low ionization energy coupled with low compensation allowed for nearly complete Si ionization at moderate temperatures. A room temperature conductivity  $>1~\Omega^{-1}\,\mathrm{cm}^{-1}$  and free carrier concentration as high as  $5\times10^{18}\,\mathrm{cm}^{-3}$  were achieved.

The authors acknowledge funding in part from AFOSR (Nos. FA9550-17-1-0225 and FA9550-19-1-0114), NSF (Nos. ECCS-1508854, ECCS-1610992, DMR-1508191, and ECCS-1653383), ARO (Nos. W911NF-15-2-0068 and W911NF-16-C-0101), and DOE (No. DE-SC0011883).

#### **DATA AVAILABILITY**

The data that support the findings of this study are available within this article.

#### REFERENCES

- <sup>1</sup>E. Silveira, J. A. Freitas, S. B. Schujman, and L. J. Schowalter, J. Cryst. Growth 310, 4007 (2008).
- <sup>2</sup>Q. Guo and A. Yoshida, Jpn. J. Appl. Phys., Part 1 33, 2453 (1994).
- <sup>3</sup>H. Morkoç, Handbook of Nitride Semiconductors and Devices, Materials Properties, Physics and Growth (John Wiley & Sons, 2009).
- <sup>4</sup>T. Kinoshita, T. Nagashima, T. Obata, S. Takashima, R. Yamamoto, R. Togashi, Y. Kumagai, R. Schlesser, R. Collazo, A. Koukitu, and Z. Sitar, Appl. Phys. Express 8, 061003 (2015).
- <sup>5</sup>P. Reddy, I. Bryan, Z. Bryan, J. Tweedie, R. Kirste, R. Collazo, and Z. Sitar, J. Appl. Phys. **116**, 194503 (2014).
- <sup>6</sup>R. Zeisel, M. W. Bayerl, S. T. B. Goennenwein, R. Dimitrov, O. Ambacher, M. S. Brandt, and M. Stutzmann, Phys. Rev. B 61, R16283 (2000).
- <sup>7</sup>Y. Taniyasu, M. Kasu, and T. Makimoto, Appl. Phys. Lett. **85**, 4672 (2004).
- <sup>8</sup>E. C. H. Kyle, S. W. Kaun, P. G. Burke, F. Wu, Y.-R. Wu, and J. S. Speck, J. Appl. Phys. 115, 193702 (2014).
- <sup>9</sup>I. Bryan, Z. Bryan, S. Washiyama, P. Reddy, B. Gaddy, B. Sarkar, M. H. Breckenridge, Q. Guo, M. Bobea, J. Tweedie, S. Mita, D. Irving, R. Collazo, and Z. Sitar, Appl. Phys. Lett. **112**, 062102 (2018).
- <sup>10</sup> K. Nakano, M. Imura, G. Narita, T. Kitano, Y. Hirose, N. Fujimoto, N. Okada, T. Kawashima, K. Iida, K. Balakrishnan, M. Tsuda, M. Iwaya, S. Kamiyama, H. Amano, and I. Akasaki, Phys. Status Solidi A 203, 1632 (2006).
- <sup>11</sup>H. Hirayama, S. Fujikawa, N. Noguchi, J. Norimatsu, T. Takano, K. Tsubaki, and N. Kamata, Phys. Status Solidi A 206, 1176 (2009).
- <sup>12</sup>J. Bai, M. Dudley, W. H. Sun, H. M. Wang, and M. A. Khan, Appl. Phys. Lett. 88, 051903 (2006).
- <sup>13</sup>H. Miyake, G. Nishio, S. Suzuki, K. Hiramatsu, H. Fukuyama, J. Kaur, and N. Kuwano, Appl. Phys. Express 9, 025501 (2016).
- <sup>14</sup>S. F. Chichibu, H. Miyake, Y. Ishikawa, M. Tashiro, T. Ohtomo, K. Furusawa, K. Hazu, K. Hiramatsu, and A. Uedono, J. Appl. Phys. 113, 213506 (2013).
- <sup>15</sup>M. Feneberg, B. Neuschl, K. Thonke, R. Collazo, A. Rice, Z. Sitar, R. Dalmau, J. Xie, S. Mita, and R. Goldhahn, Phys. Status Solidi A 208, 1520 (2011).
- Ale, S. Mita, and R. Goldmann, Phys. Status Solidi A 208, 1520 (2011).

  16R. Collazo, S. Mita, J. Xie, A. Rice, J. Tweedie, R. Dalmau, and Z. Sitar, Phys. Status Solidi C 8, 2031 (2011).
- <sup>17</sup>R. Dalmau, B. Moody, R. Schlesser, S. Mita, J. Xie, M. Feneberg, B. Neuschl, K. Thonke, R. Collazo, A. Rice, J. Tweedie, and Z. Sitar, J. Electrochem. Soc. 158, H530 (2011)
- <sup>18</sup>M. H. Breckenridge, Q. Guo, A. Klump, B. Sarkar, Y. Guan, J. Tweedie, R. Kirste, S. Mita, P. Reddy, R. Collazo, and Z. Sitar, Appl. Phys. Lett. 116, 172103 (2020).

- <sup>19</sup>M. Kanechika and T. Kachi, Appl. Phys. Lett. **88**, 202106 (2006).
- <sup>20</sup>C. G. V. de Walle and J. Neugebauer, J. Appl. Phys. **95**, 3851 (2004).
- <sup>21</sup>S. Mita, R. Collazo, A. Rice, R. F. Dalmau, and Z. Sitar, J. Appl. Phys. **104**, 013521 (2008).
- <sup>22</sup>F. Mehnke, X. T. Trinh, H. Pingel, T. Wernicke, E. Janzén, N. T. Son, and M. Kneissl, J. Appl. Phys. **120**, 145702 (2016).
- <sup>23</sup>F. Kaess, S. Mita, J. Xie, P. Reddy, A. Klump, L. H. Hernandez-Balderrama, S. Washiyama, A. Franke, R. Kirste, A. Hoffmann, R. Collazo, and Z. Sitar, J. Appl. Phys. 120, 105701 (2016).
- <sup>24</sup>Y. Cao, R. Chu, R. Li, M. Chen, R. Chang, and B. Hughes, Appl. Phys. Lett. 108, 062103 (2016).
- <sup>25</sup>N. A. Fichtenbaum, T. E. Mates, S. Keller, S. P. DenBaars, and U. K. Mishra, J. Cryst. Growth 310, 1124 (2008).
- <sup>26</sup>A. Saxler, D. Walker, P. Kung, X. Zhang, M. Razeghi, J. Solomon, W. C. Mitchel, and H. R. Vydyanath, Appl. Phys. Lett. 71, 3272 (1997).
- <sup>27</sup>P. Reddy, S. Washiyama, F. Kaess, R. Kirste, S. Mita, R. Collazo, and Z. Sitar, J. Appl. Phys. **122**, 245702 (2017).
- <sup>28</sup>S. Washiyama, P. Reddy, B. Sarkar, M. H. Breckenridge, Q. Guo, P. Bagheri, A. Klump, R. Kirste, J. Tweedie, S. Mita, Z. Sitar, and R. Collazo, J. Appl. Phys. 127, 105702 (2020).
- <sup>29</sup>P. Reddy, M. P. Hoffmann, F. Kaess, Z. Bryan, I. Bryan, M. Bobea, A. Klump, J. Tweedie, R. Kirste, S. Mita, M. Gerhold, R. Collazo, and Z. Sitar, J. Appl. Phys. 120, 185704 (2016).
- 30 K. Alberi and M. A. Scarpulla, Sci. Rep. 6, 27954 (2016).
- <sup>31</sup>Z. Bryan, M. Hoffmann, J. Tweedie, R. Kirste, G. Callsen, I. Bryan, A. Rice, M. Bobea, S. Mita, J. Xie, Z. Sitar, and R. Collazo, J. Electron. Mater. 42, 815 (2013).
- 32Z. Bryan, I. Bryan, B. E. Gaddy, P. Reddy, L. Hussey, M. Bobea, W. Guo, M. Hoffmann, R. Kirste, J. Tweedie, M. Gerhold, D. L. Irving, Z. Sitar, and R. Collazo, Appl. Phys. Lett. 105, 222101 (2014).
- <sup>33</sup>M. P. Hoffmann, J. Tweedie, R. Kirste, Z. Bryan, I. Bryan, M. Gerhold, Z. Sitar, and R. Collazo, SPIE Proc. 8986, 89860T (2014).
- <sup>34</sup>M. P. Hoffmann, Polarity Control and Doping in Aluminum Gallium Nitride (Technische Universität Berlin, 2013).
- 35J. S. Tweedie, X-Ray Characterization and Defect Control of III-Nitrides (North Carolina State University, 2012).
- <sup>36</sup>M. Ichimura, T. Wada, S. Fujita, and S. Fujita, Jpn. J. Appl. Phys., Part 1 30, 3475 (1991).
- <sup>37</sup>Z. G. Herro, D. Zhuang, R. Schlesser, R. Collazo, and Z. Sitar, J. Cryst. Growth 286, 205 (2006).
- <sup>38</sup>D. Zhuang, Z. G. Herro, R. Schlesser, and Z. Sitar, J. Cryst. Growth **287**, 372 (2006).
- <sup>39</sup>P. Lu, R. Collazo, R. F. Dalmau, G. Durkaya, N. Dietz, B. Raghothamachar, M. Dudley, and Z. Sitar, J. Cryst. Growth 312, 58 (2009).
- <sup>40</sup>I. Bryan, A. Rice, L. Hussey, Z. Bryan, M. Bobea, S. Mita, J. Xie, R. Kirste, R. Collazo, and Z. Sitar, Appl. Phys. Lett. 102, 061602 (2013).
- <sup>41</sup>F. Kaess, P. Reddy, D. Alden, A. Klump, L. H. Hernandez-Balderrama, A. Franke, R. Kirste, A. Hoffmann, R. Collazo, and Z. Sitar, J. Appl. Phys. 120, 235705 (2016).
- <sup>42</sup>R. France, T. Xu, P. Chen, R. Chandrasekaran, and T. D. Moustakas, Appl. Phys. Lett. **90**, 062115 (2007).
- <sup>43</sup>B. B. Haidet, B. Sarkar, P. Reddy, I. Bryan, Z. Bryan, R. Kirste, R. Collazo, and Z. Sitar, Jpn. J. Appl. Phys., Part 1 56, 100302 (2017).
- 44 J. L. Lyons, A. Janotti, and C. G. Van de Walle, Phys. Rev. B 89, 035204 (2014).
- <sup>45</sup>D. Alden, J. S. Harris, Z. Bryan, J. N. Baker, P. Reddy, S. Mita, G. Callsen, A. Hoffmann, D. L. Irving, R. Collazo, and Z. Sitar, Phys. Rev. Appl. 9, 054036 (2018).
- <sup>46</sup>J. S. Harris, J. N. Baker, B. E. Gaddy, I. Bryan, Z. Bryan, K. J. Mirrielees, P. Reddy, R. Collazo, Z. Sitar, and D. L. Irving, Appl. Phys. Lett. 112, 152101 (2018).
- <sup>47</sup>P. Reddy, F. Kaess, J. Tweedie, R. Kirste, S. Mita, R. Collazo, and Z. Sitar, Appl. Phys. Lett. 111, 152101 (2017).
- 48P. Reddy, I. Bryan, Z. Bryan, J. Tweedie, S. Washiyama, R. Kirste, S. Mita, R. Collazo, and Z. Sitar, Appl. Phys. Lett. 107, 091603 (2015).
- <sup>49</sup>P. Reddy, I. Bryan, Z. Bryan, W. Guo, L. Hussey, R. Collazo, and Z. Sitar, J. Appl. Phys. 116, 123701 (2014).